MONTHLY NOTICES of the Royal Astronomical Society

New quantitative nitrogen abundance estimations in a sample of Seyfert 2 Active Galactic Nuclei

Journal:	*Monthly Notices of the Royal Astronomical Society*
Manuscript ID	MN-17-0207-L.R2
Manuscript type:	Letter
Date Submitted by the Author:	08-Mar-2017
Complete List of Authors:	Dors Junior, Oli; UNIVAP, IP&D Arellano-Córdova, Karla; Instituto Nacional de Astrofísica, Óptica y Electrónica, Astrofísica Cardaci, Mónica Hagele, Guillermo; Instituto de Astrofísica de La Plata, CONICET, ; Universidad Nacional de La Plata, Facultad de Ciencias Astronómicas y Geofísicas
Keywords:	galaxies: abundances < Galaxies, galaxies: active < Galaxies, galaxies: evolution < Galaxies, galaxies: ISM < Galaxies, galaxies: nuclei < Galaxies, galaxies: Seyfert < Galaxies

Mon. Not. R. Astron. Soc. **000**, 1–6 (2011) Printed 8 March 2017 (MN LATEX style file v2.2)

New quantitative nitrogen abundance estimations in a sample of Seyfert 2 Active Galactic Nuclei

O. L. Dors Jr.[1⋆], K. Z. Arellano-Córdova[2], M. V. Cardaci[3,4], G. F. Hägele[3,4],
[1] *Universidade do Vale do Paraíba, Av. Shishima Hifumi, 2911, Cep 12244-000, São José dos Campos, SP, Brazil*
[2] *Instituto Nacional de Astrofísica, Óptica y Electrónica (INAOE), Apdo. Postal 51 y 216, Puebla, Mexico*
[3] *Instituto de Astrofísica de La Plata (CONICET-UNLP), Argentina.*
[4] *Facultad de Ciencias Astronómicas y Geofísicas, Universidad Nacional de La Plata, Paseo del Bosque s/n, 1900 La Plata, Argentina.*

Accepted 2015 Month 00. Received 2015 Month 00; in original form 2014 December 17

ABSTRACT

We obtained new quantitative determinations of the nitrogen abundance and a consistent relation between nitrogen and oxygen abundances for a sample of Seyfert 2 galaxies located at redshift $z < 0.1$. We carried out this analysis using the CLOUDY code to build detailed photoionization models. We were able to reproduce observed optical narrow emission line intensities for 44 sources compiled from the literature. Our results show that Seyfert 2 nuclei have nitrogen abundances ranging from ~ 0.3 to ~ 7.5 times the solar value. We derived the relation $\log(\mathrm{N/H}) = 1.05(\pm0.09) \times [\log(\mathrm{O/H})] - 0.35(\pm0.33)$. Results for N/O vs. O/H abundance ratios derived for Seyfert 2 galaxies are in consonance with those recently derived for a sample of extragalactic disk H II regions with high metallicity.

Key words: galaxies: active – galaxies: abundances – galaxies: evolution – galaxies: nuclei – galaxies: formation– galaxies: ISM – galaxies: Seyfert

1 INTRODUCTION

The spectra of Active Galactic Nuclei (AGNs) present strong emission lines of heavy elements that are easily measured, even in objects at high redshifts. The line intensities can be used to estimate the metallicity of these objects. Therefore, AGN metallicity determinations play a fundamental role in the knowledge of the chemical evolution of galactic nuclei (e.g. Dors et al. 2014; Matsuoka et al. 2009; Nagao et al. 2006). They also provide an indirect understanding of the star formation history for the central parts of galaxies (Hamann & Ferland 1992, 1993; Collin & Zahn 1999; Wang et al. 2011).

The first abundance determinations based on optical emission lines in AGNs were carried out by Osterbrock & Miller (1975) for the radio galaxy 3C 405 (Cygnus A). These authors calculated the abundances of helium and of other heavy elements (relative to the hydrogen abundance) through determinations of the electron temperature of the AGN gas, i.e. using the T_e – method (e.g. Peimbert & Costero 1969). Osterbrock and collaborators, with the goal of increasing the sample, produced a spectrophotometric survey of radio galaxies obtaining the physical conditions of the nuclear gas of several objects. Results of this analysis were published by Costero & Osterbrock (1977) and Koski (1978). After these pioneer works, several authors have addressed efforts in order to determine chemical abundances in AGNs (see Hamann & Ferland 1999 and references therein). However, most of these works have considered only the metallicity parametrized through the oxygen abundance determinations (e.g. Dors et al. 2015, 2014; Richardson et al. 2014; Matsuoka et al. 2009; Nagao et al. 2006; Groves et al. 2006; Storchi-Bergmann et al. 1998; Cruz-Gonzalez et al. 1991).

In particular, the knowledge of the nitrogen abundances in ionized nebulae and AGNs is essential for the study of chemical evolution of galaxies, stellar nucleosynthesis and stellar material ejection in the interstellar medium. This also helps to verify the presence of Wolf-Rayet stars in metal rich environments. Nitrogen abundances are well-known in star-forming regions. In fact, studies based on spectroscopic data of H II regions have shown that this element has a primary origin for the low metallicity regime ($[12 + \log(\mathrm{O/H})] \lesssim 8.2$) and a secondary one for the high metallicity regime (e.g. Edmunds 1990; Pérez-Montero & Contini 2009; Pilyugin & Thuan 2011). However, nitrogen abundances are poorly known in AGNs and most abundance determinations of this element in these objects are qualitative. Storchi-Bergmann & Pastroriza (1990) compared the intensity of the

⋆ E-mail:olidors@univap.br

[N II](λλ6548,6584)/Hα and [S II](λλ6716,31)/Hα ratios predicted by photoionization models with observational data from a sample of 177 Seyfert 2 galaxies (hereafter Sy2s). These authors found that models assuming nitrogen abundances ranging from 0.5 to 3 times the solar values reproduce the observational data (see also Yu & Hwang 2011; Bradley, Kaiser & Baan 2004). Moreover, the majority of the photoionization models built in order to reproduce AGN emission line intensities assumed a N/O-O/H relation derived from H II region abundance determinations (Dors et al. 2015, 2014; Matsuoka et al. 2009; Groves et al. 2006; Nagao et al. 2006). If these relations are not valid for AGN, incorrect metallicity determinations or calibrations between metallicity and strong emission-lines could be obtained (Pérez-Montero & Contini 2009).

In this letter, we present a new quantitative nitrogen abundance determinations (relative to the hydrogen abundances) for a sample of Sy2s, making also possible to obtain the N/H-O/H relation for these objects. For this purpose, we compiled optical narrow emission line intensities from the literature and we built detailed photoionization models to reproduce the observational data of each object of the sample. In Section 2 we describe the observational data. In Section 3 we present the photoionization model description and the methodology used to fit the detailed models to the observational data. In Sections 4 and 5 we present our results and conclusions, respectively.

2 AGN SAMPLE

We compiled from the literature narrow emission line intensities of AGNs classified as Seyfert 2 and 1.9 observed in the optical range (3000 Å $<\lambda<$ 7000 Å). In general, Seyfert 1 nuclei present a secondary source of ionization and heating, i.e. shocks with high velocity, not considered by the Cloudy code. Therefore, these objects were not considered in our sample.

We established as selection criterion the presence of the [O II]λλ3726+29 (hereafter [O II]λ3727), [O III]λ5007, [N II]λ6584 and [S II]λλ6716+31 narrow emission lines with full width at half-maximum (FWHM) lower than 1000 km/s. The sample consists of 47 Sy2 nuclei compiled by Dors et al. (2015) and 14 observed by Dopita et al. (2015). All emission line intensities are reddening corrected. The AGN sample is composed of objects with redshift $z \lesssim 0.1$, observed with long-slit spectroscopy and with integral-field spectroscopy, i.e. an heterogeneous sample. Castro et al. (2017) and Dors et al. (2015) showed that no bias is introduced in chemical abundance studies if heterogeneous sample of data is considered. In Table 1, we list the object identification, the observational and model predicted emission line intensities (relative to Hβ=1.0), redshift values taken from NED [1], and the references from which the data were taken.

[1] The NASA/IPAC Extragalactic Database (NED) is operated by the Jet Propulsion Laboratory, California Institute of Technology, under contract with the National Aeronautics and Space Administration.

3 PHOTOIONIZATION MODEL

3.1 Initial parameters

We used the Cloudy code version 13.04 (Ferland et al. 2013) to build individual photoionization models in order to reproduce the observed emission line intensities for each object of our sample. For each object, we built a first model assuming the following initial parameters:

(i) Number of ionizing photons [Q(H)]– The logarithm of the number of ionizing photons was considered to be equal to 51 dex, a typical value derived for Seyfert galaxies (Riffel et al. 2009).

(ii) Spectral Energy Distribution (SED)– The SED of the ionizing source was modelled as a power law of the form $F_\nu \sim \nu^\alpha$, where α was assumed to be equal to $\alpha = -1.4$, a typical value for AGNs (e.g. Zamorani et al. 1981).

(iii) Electron density (N_e)– We assume a constant value for the electron density N_e along the radius of the hypothetical AGN emission region. This value was derived, for each object, by using the observed [S II]λ6716/λ6731 ratio, obtained from the original work from which the observational data were taken (see Table 1), and using its relation with N_e obtained by Hägele et al. (2008).

(iv) Inner and outer radius– The inner radius (R_{in}), defined as being the distance from the ionizing source to the illuminated gas region, was considered to be equal to 3 pc, a typical value for narrow line regions of Seyfert galaxies (e.g. Balmaverde et al. 2016). The outer radius was assumed to be the one where the electron temperature of the gas reaches 4 000 K, the default lowest-allowed kinetic temperature by the Cloudy code. Gas cooler than ∼4 000 K does practically not emit optical emission lines.

(v) Metallicity (Z)– For each model, we assume an initial value of Z obtained from the calibration proposed by Castro et al. (2017):

$$(Z/Z_\odot) = 1.08(\pm0.19) \times x^2 + 1.78(\pm0.07) \times x + 1.24(\pm0.01),$$

being $x = \log$ ([N II]λ6584/[O II]λ3727) calculated from the observational data listed in Table 1.

(vi) Nitrogen and sulphur abundances– The nitrogen (N/H) and sulphur (S/H) abundances relative to the hydrogen abundance were considered to be 2 and 1 times the solar values, respectively. In the Cloudy code the solar values $12+\log(N/H)_\odot$=7.93 and $12+\log(S/H)_\odot$ = 7.27 were taken from Holweger (2001) and Grevesse & Sauval (1998), respectively.

3.2 Fitting model methodology

An initial model assuming the input parameters described in Section 3.1 was built in order to reproduce the emission line intensities of each object of the sample. Then, we ran new models varying separately, the Z, N/H, S/H values considering a step of ±0.2 dex, typical uncertainty in nebular abundance estimations derived through photoionization models (Dors et al. 2011). From this series of models, we selected one that best reproduces the intensities of all emission lines considered (see Sect. 2) within an uncertainty of ±20%, which is a typical observational uncertainty for emission lines (e.g. Kraemer et al. 1994). If no model was able to reach this criterion, a new series of models was built varying N_e, R_{in}

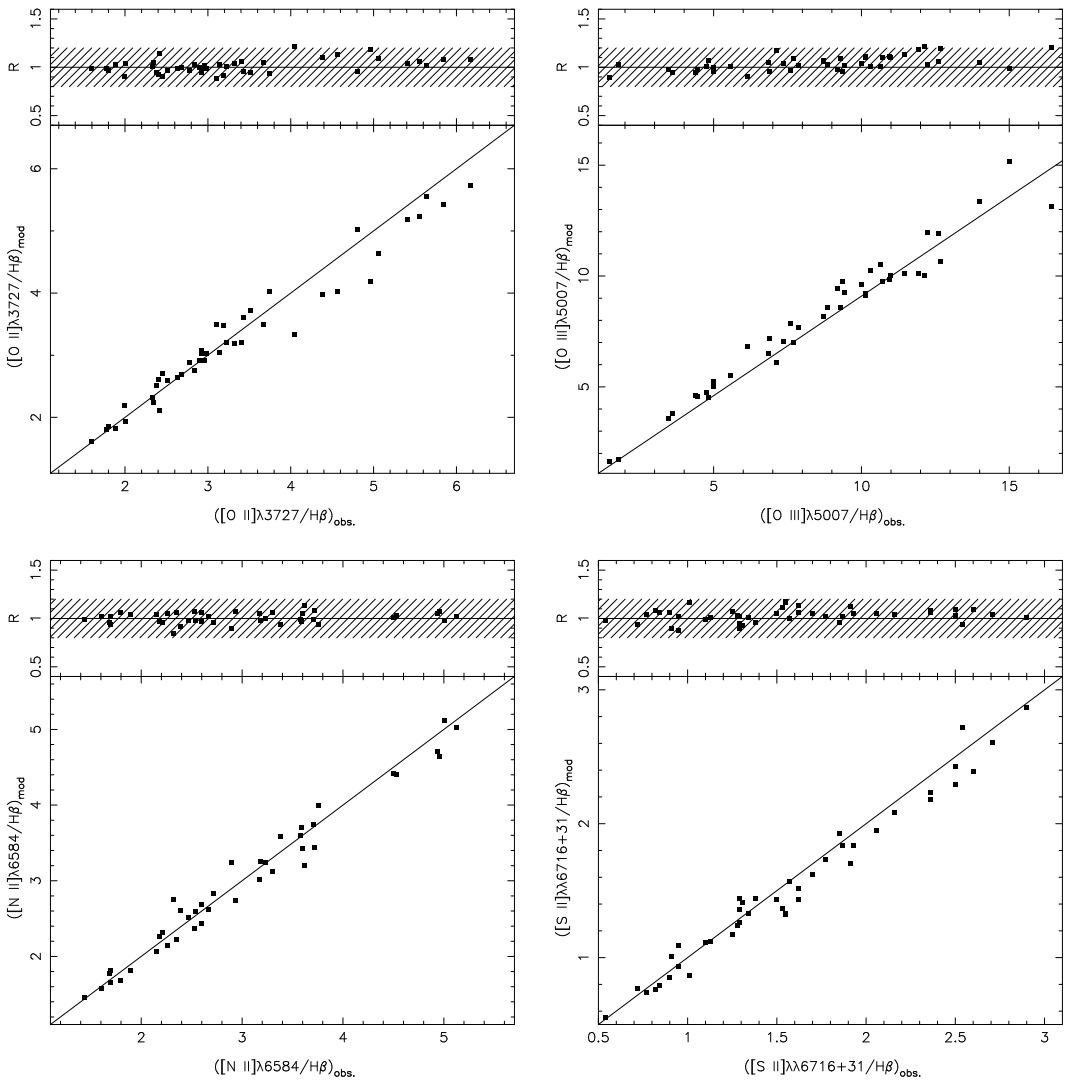

Figure 1. Bottom part of each panel: comparison between model predicted and observed emission line intensities (with respect to Hβ) for the sample of Sy2s (see Sect 4). Solid lines represent equality of the two estimates. Top part of each panel: ratio between the observed and predicted intensities of a given emission line versus the observed emission line intensity for the same ratio. The hatched area indicates the band of 20% adopted for the agreement between the observed and predicted emission line intensities (see Sect. 3.2).

and α with a step of $\pm$0.2 dex. Only one parameter was varied at a time and the optimization method PHYMIR (van Hoof 1997) was considered to select the best fitting model to the set of emission line intensities. Similar methodology was adopted by Dors et al. (2011) in a study of chemical abundances in H II regions.

To determine the error in our abundance estimations, a simple model simulation was performed. Initially, we built a photonionization model assuming solar metallicity, $N_{\rm e}$=500 cm^{-3} (typical electron density value derived for AGNs, see Dors et al. 2015), and the initial parameters listed above. Thereafter, a series of models varying the O/H, N/H and S/H abundances by a factor of $\pm$0.5 dex (step of 0.05 dex) from the solar values was built. Using these models, we obtained an abundance range for which emission line intensities differ $\pm$20% from the values predicted by the initial model. We found that a variation of about $\pm$0.1 dex in abundances yields variations of about 20% in the intensities of the emission lines considered. This value will be considered as the uncertainty in our abundance estimations.

4 RESULTS AND DISCUSSION

From the 61 objects in our sample, it was possible to obtain detailed photoionization model solutions for 44 of them. The predicted emission line intensities and the final model parameters for these 44 objects are listed in Table 1 and 2, respectively.

In Fig. 1, bottom part of each panel, the observational emission line intensities (with respect to Hβ) are compared with those predicted by the detailed photoionization models, for each of the 44 fitted object of the sample. Also in Fig. 1, top part of each panel, the ratio between the observed and the modelled intensities as a function of the observed ones is shown. We can note that, for most cases, the larger

Table 1. Dereddened fluxes (relative to Hβ=1.00) for a sample of Seyfert 2 nuclei. The observed values compiled from the literature are referred as "Obs." while the predicted values by the photoionization models as "Mod." (see Sect. 3 of the Letter). The redshift and the references of the compiled sample (given below) are presented in the last columns, respectively. The redshift values were taken from the NASA/IPAC Extragalactic Database (NED). Full table is available online.

	[O II]$\lambda\lambda$3726,29		[O III]λ5007		[N II]λ6584		[S II]$\lambda\lambda$6716+31		redshift	Ref.
Object	Obs.	Mod.	Obs.	Mod.	Obs.	Mod.	Obs.	Mod.		
IZw 92	2.63	2.65	10.12	9.19	0.97	1.01	0.77	0.74	0.0378	1
NGC 3393	2.41	2.61	16.42	13.15	4.50	4.42	1.53	1.37	0.0125	2

Table 2. Assumed model parameter values used to fit the emission lines observed in the 44 modeled Seyfert 2 nuclei. Full table is available online.

Object	log(O/H)	log(N/H)	log(S/H)	N_e (cm^3)	log[Q(H)]	α
IZw 92	−3.4256	−4.1850	−4.9190	822	51.27	−1.4
NGC 3393	−3.0583	−3.4935	−4.3300	4162	50.55	−1.0

discrepancy is derived for the [O III]λ5007/Hβ ratio, where the intensities observed are, in general, higher than those predicted by the models. This could be due to the presence of a secondary source of ionization and heating in the AGNs (not considered in the photoionization models) producing a more pronounced increase in the [O III] line intensities; hence, these emission lines have a strong dependence with the electron temperature (see also Dors et al. 2015; Pérez-Montero et al. 2010). Moreover, the supposition of electron density constant along the radius of the narrow line region, do not treat all the relevant physical processes correctly (e.g. process of gas cooling by free-free and free-bound emission, or temperature fluctuations), and the used of simplified geometry in the models, could also be responsible for this discrepancy.

In Fig. 2, we present a histogram containing the oxygen and nitrogen abundances relative to the hydrogen abundance, predicted by our photoionization models for the 44 fitted objects of our sample (listed in Table 2). Analysing the obtained oxygen abundance distribution, we found that $\sim 70\%$ of the objects present O/H abundances in the range $8.6 \lesssim 12 + \log(\mathrm{O/H}) \lesssim 9.0$ (or metallicities in the range $1.0 \lesssim (Z/Z_\odot) \lesssim 2.0$). This result is in consonance with the results found by Castro et al. (2017) and Dors et al. (2015), who considered a different methodology to estimate the metallicity for a similar sample of objects.

Regarding the nitrogen abundance distribution also presented in Fig. 2, we found that Sy2 nuclei exhibit a wide range of N/H abundances, i.e. $7.4 \lesssim 12 + \log(\mathrm{N/H}) \lesssim 8.8$ or, $0.3 \lesssim (\mathrm{N/N_\odot}) \lesssim 7.4$. This is a wider range of values than the one derived by Storchi-Bergmann & Pastroriza (1990). The discrepancy between these estimations is probably due to differences in the studied sample or due to differences in the employed methodology.

Our abundance results make possible to derive a relation between nitrogen and oxygen abundances in Sy2s. With this goal, in Fig. 3, we show log(N/H) versus log(O/H) (listed in Table 2). We see a clear correlation indicating that the nitrogen has a secondary origin for $12+\log(\mathrm{O/H}) > 8.0$, in Sy2 nuclei. A linear regression fitting these data produce:

$$\log(\mathrm{N/H}) = (1.05 \pm 0.09) \times [\log(\mathrm{O/H})] - (0.35 \pm 0.33).$$

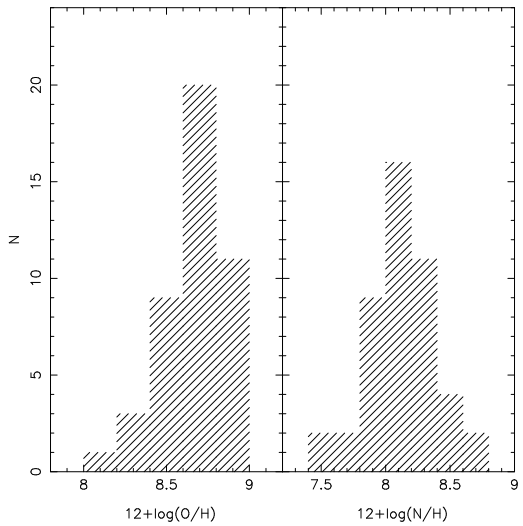

Figure 2. Histogram containing the oxygen (left panel) and nitrogen (right panel) abundance distributions predicted by our photoionization models for the 44 fitted objects of our sample (see Sect. 4).

In Fig. 4, the predicted N/O as a function of O/H values for the AGN sample is compared with those derived for a sample of H II regions by Pilyugin & Grebel (2016), who used the C-method (Pilyugin et al. 2012) to calculate the oxygen and nitrogen abundances. In this plot, the value for the solar abundance is also indicated. We can see that the N/O estimations for the Sy2 objects are in agreement with those for the metal richest H II regions. Moreover, the N/O values of the objects of our sample are, in most cases, higher than the solar value.

5 CONCLUSION

We compiled from the literature narrow optical emission line intensities for a sample of Seyfert 2 galaxies. Standard photoionization models were built in order to reproduce the intensities of these emission lines. We present new results of

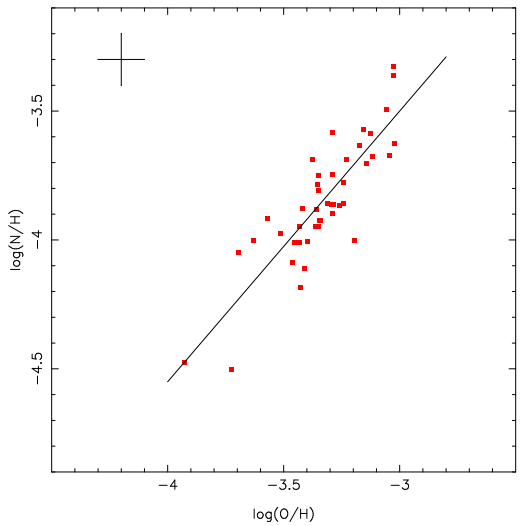

Figure 3. log(N/H) vs. log(O/H) predicted by the models. The line represents a linear regression fitting the points, given by $\log(N/H) = (1.05 \pm 0.09) \times [\log(O/H)] - (0.35 \pm 0.33)$. Error bars represents the uncertainty 0.2 dex in our abundance estimations (see Sect. 3.2).

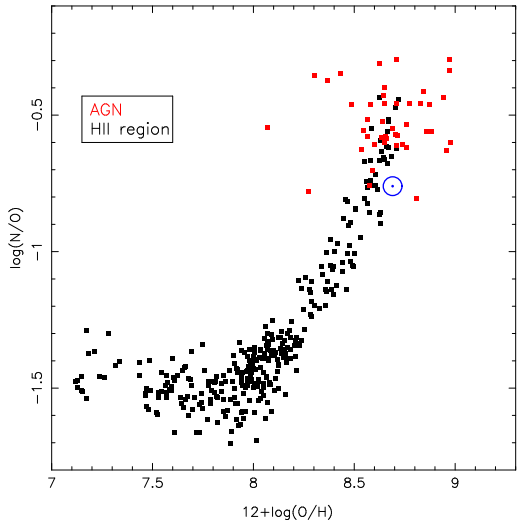

Figure 4. log(N/O) vs. 12+log(O/H) abundance ratio values. The red points are values predicted by the individual photoionization models for our sample of Sy2 objects (see Sect. 4), while the black points are estimations for H II regions derived by Pilyugin & Grebel (2016) using the C-method (Pilyugin et al. 2012). The value for the solar ratio abundance taken from Holweger (2001) and Grevesse & Sauval (1998) is also indicated in the plot with a blue symbol.

nitrogen and oxygen abundances calculated for a large sample of Seyfert 2 galaxies. We found a very wide range for the N/H abundances in this kind of active nuclei, varying between about 0.3 and 7.5 times the solar value. We derived a relationship between the nitrogen and oxygen abundances for Seyfert 2 AGNs. We find that N/O abundance ratios in Seyfert 2 galaxies are similar to those recently derived for a sample of extragalactic H II regions with high metallicity.

ACKNOWLEDGMENTS

We are grateful to the referee, Dra Marcella Contini, for her useful comments and suggestions, which have helped us to substantially clarify and improve the manuscript. O.L.D. is grateful to FAPESP (2016/04728-7) and CNPQ (306744/2014-7).

REFERENCES

Adelman-McCarthy J. K. et al., 2006, ApJS, 162, 38
Alloin D., Bica E., Bonatto C., Prugniel P., 1992, A&A, 266, 117
Baldwin J. A., Hamann F., Korista K. T., Ferland G. J., Dietrich M., Warner C., 2003, ApJ, 583, 649
Batra N. D., & Baldwin J. A., 2014, MNRAS, 439, 771
Balmaverde B. et al., 2016, A&A, 586, 48
Bradley L. D., Kaiser M. E., Baan W. A., 2004, ApJ, 603, 463
Castro C. S., Dors O. L., Cardaci M. V., Hägele G. F., 2017, MNRAS, arXiv:1701.04997
Cohen R. D., 1983, ApJ, 273, 489
Collin S., & Zahn, J.-P., 1999, Ap&SS, 265, 501
Contini M., 2012, MNRAS, 425, 1205
Costero R., & Osterbrock, 1977, ApJ, 211, 675
Cruz-Gonzalez I., Guichard J., Serrano A., Carrasco L., 1991, PASP, 103, 888
Dopita M. A. et al., 2015, ApJS, 217, 12
Dopita M. A., Kewley L. J., Heisler C. A., Sutherland R. S., 2000, ApJ., 542, 224
Dopita M. A., 1995, Ap&SS, 233, 215
Dors O. L. et al., 2015, MNRAS, 453, 4102
Dors O. L., Cardaci, M. V., Hägele G. F., Krabbe A. C., 2014, 443, 1291
Dors O. L., Krabbe A. C, Hägele G. F., Pérez-Montero E., 2011, MNRAS, 415, 3616
Durret F., & Bergeron J., 1988, ApJSS, 75, 273
Edmunds M. G., 1990, MNRAS, 246, 678
Ferland G. J., 2013, Rev. Mex. Astron. Astrofis., 49, 137
Goodrich R. W., & Osterbrock D., 1983, ApJ, 269, 416
Grevesse N., & Sauval A. J., 1998, SSrv, 85, 161
Groves B. A., Heckman T. M., Kauffmann G., 2006, MNRAS, 371, 1559
Hägele G. F., Díaz A. I., Terlevich E., Terlevich R., Pérez-Montero E., Cardaci M. V., 2008, MNRAS, 383, 209
Hamann F., & Ferland G., 1999, ARA&A, 37, 48
Hamann F., & Ferland G., 1992, ApJ, 391, L53
Hamann F., & Ferland G., 1993, ApJ, 418, 11
Holweger H., 2001, in Wimmer-Schweingruber R. F., ed., Joint SOHO/ACE workshop "Solar and Galactic Composition" Vol. 598 of American Institute of Physics Conference Series, Photospheric abundances: Problems, updates, implications. pp 23-30
Koski A. T., 1978, ApJ, 223, 56
Kraemer S. B., Wu C.-C., Crenshaw D. M., Harrington J. P., 1994, ApJ, 435, 171
Matsuoka K., Nagao T., Maiolino R., Marconi A., Taniguchi Y., 2009, A&A, 503, 721
Mouhcine M., & Contini T., 2002, A&A, 389, 106
Nagao T., Maiolino R., Marconi A., 2006, A&A, 447, 863
Osterbrock D. E., 1981, ApJ, 249, 462

Osterbrock D. E., & Miller J. S., 1975, ApJ, 197, 535
Peimbert M., & Costero R., 1969, BOTT, 5, 3
Pérez-Montero E., Garca-Benito R., Hägele G. F., Díaz A. I., 2010, MNRAS, 404, 2037
Pérez-Montero E., & Contini T., 2009, MNRAS, 398, 949
Phillips M. M., Charles P. A., Baldwin J. A., 1983, ApJ, 266, 485
Pilyugin L. S., & Thuan T. X., 2011, ApJ, 726, L23
Pilyugin L. S., & Grebel E. K., 2016, MNRAS, 457, 3678
Pilyugin L. S., Grebel E. K., Mattsson L., 2012, MNRAS, 424, 2316
Radovich, M., & Rafanelli, P., 1996, A&A, 306, 97
Richardson C. T., Allen J. T.; Baldwin J. A., Hewett P. C.
Riffel R. A., Storchi-Bergmann T., Dors O. L., Winge C., 2009, MNRAS, 698, 176
Schmitt H. R., Storchi-Bergmann T., Baldwin J. A., 1994, ApJ, 423, 237
Shuder J. M., 1980, ApJ, 240, 32, Ferland G. J., 2014, MNRAS, 437, 2376
Shuder J. M., & Osterbrock D. E., 1981, ApJ, 250, 55
Storchi-Bergmann T., Schmitt H. R., Calzetti D., Kinney A. L., 1998, AJ, 115, 909
Storchi-Bergmann T., & Partoriza M. G., 1990, PASP, 102, 1359
van Hoof P. A. M. Photo-ionization studies of nebulae. PhD thesis, Rijksuniversiteit Groningen, 1997
Zamorani G. et al., 1981, ApJ, 245, 357
Wang, J.-M. et al., 2011, ApJ, 739, 3
York D. G. et al., 2000, AJ, 120, 1579
Yu P.-C., & Hwang C.-Y., 2011, AJ, 142, 14

Table 1. Dereddened fluxes (relative to Hβ=1.00) for a sample of Seyfert 2 nuclei. The observed values compiled from the literature are referred as "Obs." while the predicted values by the photoionization models as "Mod." (see Sect. 3 of the Letter). The redshift and the references of the compiled sample (given below) are presented in the last columns, respectively. **The redshift values were taken from the NASA/IPAC Extragalactic Database (NED).**

	[O II]$\lambda\lambda$3726,29		[O III]λ5007		[N II]λ6584		[S II]$\lambda\lambda$6716+31		redshift	Ref.
Object	Obs.	Mod.	Obs.	Mod.	Obs.	Mod.	Obs.	Mod.		
IZw 92	2.63	2.65	10.12	9.19	0.97	1.01	0.77	0.74	0.0378	1
NGC 3393	2.41	2.61	16.42	13.15	4.50	4.42	1.53	1.37	0.0125	2
Mrk 3	3.52	3.72	12.67	10.64	3.18	3.25	1.55	1.32	0.0135	3
Mrk 573	2.92	3.07	12.12	10.02	2.47	2.52	1.55	1.33	0.0171	3
Mrk 78	4.96	4.19	11.94	10.11	2.32	2.75	1.29	1.26	0.0371	3
Mrk 34	3.43	3.60	11.46	10.11	2.18	2.26	1.62	1.43	0.0505	3
Mrk 1	2.78	2.89	10.95	9.86	2.21	2.31	1.01	0.87	0.0159	3
3c433	6.17	5.73	9.44	9.24	5.13	5.02	2.71	2.61	0.1016	3
Mrk 270	5.64	5.56	8.71	8.18	2.93	2.74	2.60	2.39	0.0104	3
3c452	4.81	5.02	6.85	6.52	3.58	3.60	1.87	1.84	0.0811	3
Mrk 198	2.51	2.60	5.56	5.49	2.26	2.14	1.57	1.57	0.0242	3
Mrk 268	3.75	4.02	4.82	4.52	4.94	4.71	2.36	2.23	0.0398	3
NGC 3227	3.22	3.21	10.73	9.73	5.01	5.12	2.50	2.29	0.0038	4
Mrk 6	2.45	2.70	10.13	9.12	1.79	1.68	1.25	1.17	0.0188	4
ESO 138 G1	2.35	2.24	8.71	8.19	0.68	0.70	0.95	0.93	0.0053	5
NGC 5643	5.55	5.23	12.61	11.92	2.90	3.24	1.62	1.52	0.0039	6
NGC 1667	11.50	9.73	9.20	9.45	6.96	7.43	2.54	2.72	0.0151	7
Mrk 609	1.80	1.86	5.00	5.25	2.60	2.69	1.10	1.11	0.0344	8
NGC 3081	2.16	2.18	12.62	10.92	2.33	2.32	1.22	1.77	0.0079	9
NGC 4388	2.68	2.69	10.63	10.52	1.44	1.46	1.28	1.24	0.0084	9
NGC 5135	2.01	1.94	4.47	4.57	2.35	2.22	0.72	0.77	0.0136	9
NGC 5728	3.41	3.21	10.98	10.01	3.71	3.74	0.82	0.76	0.0093	9
IC 5063	5.06	4.63	10.31	10.25	2.67	2.62	1.29	1.36	0.0113	9
IC 5135	4.05	3.34	6.88	7.19	3.30	3.12	0.95	1.09	0.0161	9
Mrk 744	2.38	2.51	8.84	8.60	3.62	3.20	5.66	5.41	0.0089	10
NGC 5506	2.84	2.76	7.69	7.02	2.53	2.37	1.91	1.70	0.0061	11
NGC 2110	4.38	3.97	4.76	4.73	3.76	4.00	2.90	2.87	0.0077	11
NGC 3281	2.33	2.32	7.59	7.85	2.54	2.60	1.13	1.12	0.0106	12
Akn 347	2.98	3.03	15.01	15.18	3.23	3.24	1.50	1.43	0.0224	13
UM 16	2.90	2.92	14.00	13.34	1.70	1.81	0.90	0.85	0.0579	13
Mrk 533	1.59	1.61	12.23	11.94	2.72	2.83	0.84	0.79	0.0289	13
Mrk 612	1.88	1.82	9.37	9.76	3.60	3.43	1.29	1.44	0.0204	13
NGC 613	2.42	2.11	0.51	0.56	1.70	1.66	0.91	1.01	0.0049	14
IC 1657	3.67	3.49	1.79	1.74	1.89	1.82	1.85	1.93	0.0119	14
IRAS 01475-0740	1.78	1.80	4.99	5.01	1.69	1.77	0.54	0.55	0.0180	14
IC 1816	1.99	2.19	10.00	9.61	4.53	4.41	2.16	2.08	0.0169	14
NGC 1125	3.14	3.05	6.16	6.83	2.15	2.06	1.38	1.44	0.0109	14
MCG -06-23-038	2.92	3.03	7.14	6.10	2.60	2.44	1.93	1.84	0.0152	14
IRAS 11215-2806	2.96	2.91	7.87	7.69	1.61	1.57	1.34	1.33	0.0139	14
ESO 137-G34	3.10	3.50	9.30	8.56	3.72	3.44	2.36	2.18	0.0091	14
NGC 6300	5.41	5.18	1.48	1.65	4.96	4.64	1.70	1.62	0.0036	14
ESO103-G35	3.19	3.48	7.35	7.06	3.17	3.01	2.06	1.95	0.0132	14
NGC 6926	5.84	5.42	4.38	4.63	3.59	3.70	2.50	2.43	0.0196	14
IC 1368	4.56	4.02	3.60	3.80	3.38	3.59	1.31	1.41	0.0130	14
NGC 7590	3.32	3.19	3.47	3.57	2.39	2.61	1.77	1.73	0.0052	14

References— (1) Kraemer et al. (1994), (2) Contini et al. (2012), (3) Koski (1978), (4) Cohen (1983), (5) Alloin et al. (1992) (6) Schmitt et al. (1994) (7) Radovich & Rafanelli (1996), (8) Osterbrock (1981), (9) Phillips et al. (1983), (10) Goodrich & Osterbrock (1983), (11) Shuder (1980), (12) Durret & Bergeron (1988), (13) Shuder & Osterbrock (1981), and (14) Dopita et al. (2015).

Table 2. Assumed model parameter values used to fit the emission lines observed in the 44 modeled Seyfert 2 nuclei.

Object	log(O/H)	log(N/H)	log(S/H)	N_e (cm^3)	log[Q(H)]	α
IZw 92	−3.4256	−4.1850	−4.9190	822	51.27	−1.4
NGC 3393	−3.0583	−3.4935	−4.3300	4162	50.55	−1.0
Mrk 3	−3.3488	−3.8080	−4.7135	948	50.62	−1.0
Mrk 573	−3.2427	−3.7756	−4.5677	781	50.79	−1.1
Mrk 78	−3.4326	−3.9486	−4.8580	370	51.00	−0.9
Mrk 34	−3.3406	−3.9248	−4.6626	546	50.90	−1.0
Mrk 1	−3.4195	−3.8789	−4.8448	767	51.04	−1.2
3c433	−3.3538	−3.7836	−4.5959	82	51.20	−0.5
Mrk 270	−3.4083	−4.1096	−4.7244	1027	49.76	−0.8
3c452	−3.5144	−3.9758	−4.9398	50	50.80	−0.9
Mrk 198	−3.3098	−3.8574	−4.6394	111	51.00	−1.4
Mrk 268	−3.3491	−3.7485	−4.7745	260	49.43	−1.1
NGC 3227	−3.2890	−3.5846	−4.3919	1622	50.44	−0.9
Mrk 6	−3.3486	−3.9486	−4.6495	647	51.09	−1.3
ESO 138 G1	−3.7251	−4.5041	−4.9830	684	51.38	−1.2
NGC 5643	−3.2868	−3.8632	−4.7122	141	51.49	−0.7
NGC 1667	−3.1418	−3.7034	−4.6136	281	50.06	−0.1
Mrk 609	−3.1575	−3.5715	−4.5829	239	50.80	−1.4
NGC 4388	−3.3990	−4.0067	−4.6243	343	51.79	−1.1
NGC 5135	−3.1166	−3.6782	−4.7766	492	50.11	−1.6
NGC 5728	−3.3745	−3.6860	−4.9360	606	50.93	−1.2
IC 5063	−3.4335	−4.0111	−4.8588	311	51.05	−0.8
IC 5135	−3.5678	−3.9159	−4.9932	471	50.55	−1.3
Mrk 744	−3.0237	−3.6241	−3.6259	2006	50.32	−0.4
NGC 5506	−3.3582	−3.8825	−4.5836	1034	50.26	−1.4
NGC 2110	−3.6305	−4.0039	−4.7492	1324	49.61	−1.1
NGC 3281	−3.2270	−3.6863	−4.5884	974	50.58	−1.4
Akn 347	−3.1257	−3.5861	−4.3740	758	51.69	−0.8
UM 16	−3.3456	−3.9243	−4.7710	606	51.83	−1.0
Mrk 533	−3.0260	−3.3614	−4.3697	1270	51.41	−1.1
Mrk 612	−3.0280	−3.3255	−4.3275	75	52.27	−0.9
NGC 613	−3.1932	−4.0002	−5.0909	76	48.04	−1.4
IC 1657	−3.9294	−4.4746	−5.2826	40	49.49	−1.4
IRAS 01475-0740	−3.0449	−3.6729	−4.8298	90	51.14	−1.4
IC 1816	−3.1728	−3.6320	−4.1765	8691	50.57	−1.0
NGC 1125	−3.3634	−3.9468	−4.7094	403	50.59	−1.4
MCG -06-23-038	−3.2606	−3.8675	−4.5737	949	49.91	−1.4
IRAS 11215-2806	−3.4637	−4.0886	−4.7418	532	50.84	−1.4
ESO 137-G34	−3.2886	−3.7479	−4.4847	736	50.60	−1.1
NGC 6300	−3.2935	−3.8638	−5.0185	842	48.94	−1.2
ESO103-G35	−3.2416	−3.8591	−4.5220	2449	49.97	−1.2
NGC 6926	−3.4548	−4.0114	−4.8733	506	49.24	−1.1
IC 1368	−3.6960	−4.0507	−5.1926	217	49.59	−1.3
NGC 7590	−3.2886	−3.8981	−4.8118	121	49.67	−1.4

REFERENCES

Alloin D., Bica E., Bonatto C., Prugniel P., 1992, A&A, 266, 117

Cohen R. D., 1983, ApJ, 273, 489

Contini M., 2012, MNRAS, 425, 1205

Dopita M. A. et al., 2015, ApJS, 217, 12

Durret F., & Bergeron J., 1988, ApJSS, 75, 273

Koski A. T., 1978, ApJ, 223, 56

Kraemer S. B., Wu C.-C., Crenshaw D. M., Harrington J. P., 1994, ApJ, 435, 171

Goodrich R. W., & Osterbrock D., 1983, ApJ, 269, 416

Osterbrock D. E., 1981, ApJ, 249, 462

Phillips M. M., Charles P. A., Baldwin J. A., 1983, ApJ, 266, 485

Radovich, M., & Rafanelli, P., 1996, A&A, 306, 97

Schmitt H. R., Storchi-Bergmann T., Baldwin J. A., 1994, ApJ, 423, 237

Shuder J. M., & Osterbrock D. E., 1981, ApJ, 250, 55

Shuder J. M., 1980, ApJ, 240, 32